SCBF GUSSET PLATE CONNECTION DESIGN

CHARLES W. ROEDER, DAWN E. LEHMAN, ERIC LUMPKIN, P0-CHIEN HSIAO, AND KEITH PALMER

ABSTRACT

Performance-based seismic design (PBSD) produces structures that meet multiple performance objectives. Special concentrically braced frames (SCBFs) are stiff, strong structures that meet PBSD serviceability limit states, but stable cyclic inelastic behavior is needed to satisfy PBSD life safety and collapse prevention limit states. This requires buckling, tensile yielding, and post-buckling inelastic deformation of the brace. Current SCBF design provisions attempt to ensure good inelastic performance by controlling the brace slenderness and connection geometry and by providing adequate connection resistance, but this approach is flawed. A research study was completed to develop improved PBSD models for SCBF gusset plate connection design. More than 35 full scale SCBF systems were experimentally evaluated, and numerous nonlinear analyses were completed. A proposed design procedure, which balances desirable yield mechanisms in the brace and connection and restricts undesirable failure modes, was developed. This work is summarized, and gusset plate connection design recommendations are presented.

SEISMIC BEHAVIOR OF BRACED FRAMES

Structures are designed to remain nearly elastic for small, frequent seismic events to assure serviceability, but cyclic, inelastic deformation is used to assure that the structure retains its integrity and prevents loss of life and collapse during large infrequent earthquakes. Performance based seismic design (PBSD) is a formalized procedure for meeting these multiple design objectives. Special concentrically braced frames (SCBFs) are stiff, strong structures, which easily meet serviceability limits states and provide economical seismic design, and they have special seismic design requirements intended to insure good inelastic performance. The brace provides great lateral stiffness to the frame and attracts large axial forces during an earthquake. The brace buckles in compression, yields in tension, and sustains inelastic post-buckling deformation during these severe seismic events. Plastic hinges form in the brace after buckling due to P-δ moments, and this yielding contributes to the post-buckling yield behavior. These effects lead to the one-sided axial force-deflection behavior of a brace seen in Fig. 1a, but SCBFs have braces in opposing pairs, and the resulting system has inelastic hysteretic behavior illustrated in Fig. 1b. The braces are usually attached to the other framing members by gusset plate connections such as illustrated in Fig. 2. The brace end rotation associated with brace buckling, causes large rotation demands on the gusset plate connection.

AISC Seismic Provisions have numerous SCBF design requirements, which are intended to assure good inelastic performance from the system (AISC, 2005a). Brace slenderness limits are applied to assure that it provides adequate ductility during post-buckling deformation, and additional framing system requirements balance the lateral resistance between tensile and compressive braces and control yielding in the beam due to unbalanced brace forces in V- or Inverted V-braced systems. Gusset plate connections are designed by variations of the AISC Uniform Force Method (UFM) (Thornton, 1991; AISC, 2005b), which was originally developed for wind load design. The UFM is adapted to seismic applications by designing the connection to resist the expected tensile ($R_y A_g F_y$) and compressive ($R_y A_g F_{cr}$) resistance of the brace. The expected brace resistance is much larger than the factored design load. Use of the expected brace forces for connection design is a rational design concept, but it sometimes leads to the mistaken perception that a bigger, stronger gusset plate makes a better connection. Rectangular high strength steel tubes are commonly used for the brace, and the tube is slit to slip over the gusset plate for the brace-to-gusset interface. Net section fracture of the brace may occur at the end of the slit, and net section reinforcement is often required. The tubes are normally joined to the gusset plate with fillet welds sized to develop the expected tensile resistance of the brace, and block shear must also be checked for this interface joint. The Whitmore width (Whitmore, 1950) of the gusset plate is defined at the end of the brace-to-gusset interface by projecting a 30^{o} angle from the start to the end of the bolted or welded joint, and the area associated with this

Whitmore width is used to define the area resisting the compressive buckling and tensile yield and fracture capacities of the gusset.

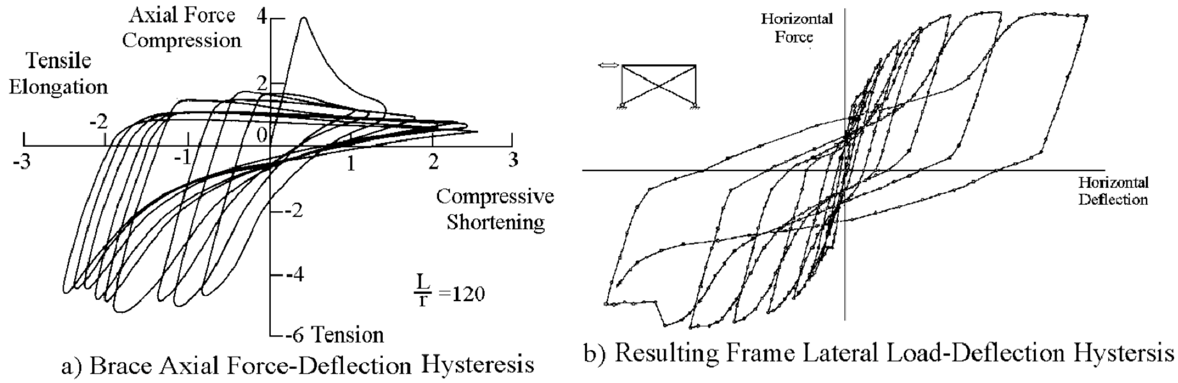

Figure 1 Behavior of Special Concentrically Braced Frames (Popov et al. 1976)

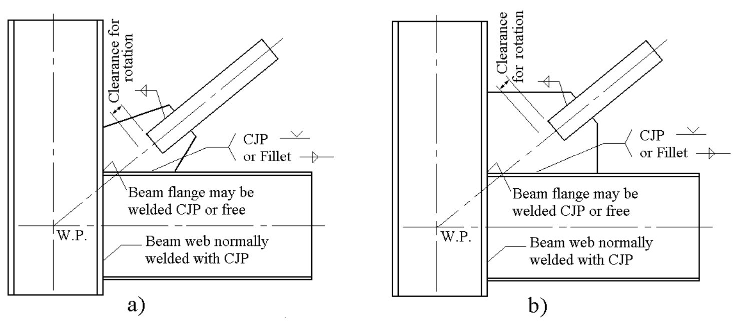

Figure 2. Schematic of Current SCBF Gusset Plate Connections; a) Tapered Gusset, b) Rectangular Gusset

Several methods have been used for evaluating the buckling capacity of the gusset plate. In some cases, edge buckling (Brown 1988, Astenah-Asl 1998) is checked, but AISC column buckling is normally evaluated with either an average gusset length (averaged based upon key points across the Whitmore width) or a centroidal length. The gusset plate must permit end rotation due to brace buckling, and this is commonly accomplished by the $2t_p$ linear clearance model illustrated in Fig. 2. This clearance model is not required, but it is a commonly used method that results in large gusset plate dimensions and consequently thicker gusset plates. Once the gusset plate geometry and thickness are defined, the bolts or welds joining the gusset plate to the beam and column are sized by the equilibrium forces associated with the UFM. Welds are often fillet welds on both sides of the plate, but complete joint penetration welds may also be employed.

The beam-column connection also affects SCBF performance. Forces that are transferred by the brace to the beam or column or by drag struts to the braced bay frequently must be transferred through this beam-column connection. There is variation in the actual practice for this part of the connection as depicted in Fig 2. Some engineers use CJP welds between the beam and column flanges to assure full force transfer (see Fig. 2a). Other engineers think that this welding is costly and unneeded, and they may use only web attachments. These combined requirements and practices result in wide variations in gusset plate connection design.

Experimental research studies on gusset plate connections have been completed (Bjorhovde and Chakrabarti, 1985; Brown, 1988; Cheng et al., 1994; Grondin et al., 2000; Hu et al., 1987; Rabinovitch and Cheng, 1993; Yam 1994; Yam and Cheng 2002). These experiments were invariably monotonic resistance tests that did not include global frame or brace buckling behaviors. Global frame and brace buckling issues have considerable impact on SCBF performance and are important concerns. Nevertheless, these past experimental results are useful in evaluating the relative accuracy of various design models. These comparisons have been made and are summarized elsewhere (Roeder et al. 2004, 2005). Most models are reasonably good but there is considerable scatter in their reliability as illustrated in Fig. 3. Figure 3a shows the measured resistance from experiments with gusset plate buckling divided by the predicted resistance from the Thornton method. The Thornton method uses the Whitmore width and an average effective buckling length of the plate over this width with effective length coefficients of 0.65

for corner gusset plates and 1.2 to 1.4 for midspan gusset plates. The ratio is plotted for all corner gusset plate connections that reported gusset buckling in past research. A ratio greater than 1.0 indicates that a conservative prediction is provided, and a ratio less than 1.0 indicates that the model overestimates the gusset plate buckling resistance. The Thornton model provides a conservative estimate the gusset plate buckling capacity with experimental resistance being 1.542 times the predicted buckling resistance and a standard deviation the ratio of 0.195. Edge buckling is also sometimes considered in gusset plate design. The model was developed by Brown (1988) with modifications by Astaneh (1989), and Fig. 3b shows the experimental comparison. The edge buckling models provide good comparisons for a few tests, but they show significantly more variability than the Thornton method, since the maximum value of ratio is larger than 7 and the minimum value is approximately 0.2. Hence, the use of the edge buckling equation is not recommended for gusset plate design by the authors.

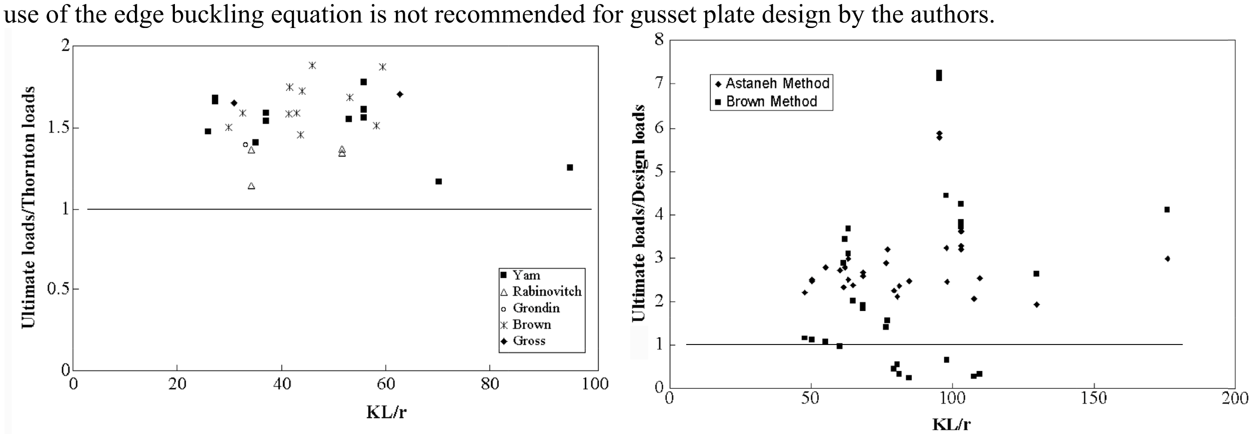

a) b)

Figure 3. Comparison of Measured Gusset Resistance to Predicted Resistance; a) Thornton Model, b) Edge Buckling Model

This introduction and summary of current design practice identifies several areas of concern for gusset plate design. First, there are inconsistencies between design model predictions and experimental results. Second, there are wide variations in design practice. Third, there are problems balancing economy and performance with issues such as net section fracture of the brace, gusset plate and brace clearance requirements, and gusset plate weld size. Fourth, while braced frames essentially are designed as trusses, the gusset plates are quite large, and they often restrain member rotation, inhibit truss action, and induce large inelastic flexural deformations into frame members. As a result of these issues, a comprehensive experimental and analytical research program on braced frame gusset plate connections was performed.

EXPERIMENTAL PROGRAM

SCBF experiments must include complete bays of an SCBF frame to fully incorporate the issues noted earlier. An experimental research program including 28 full-scale, single-bay single-story SCBFs with member sizes typical of those used in the bottom story of a 3- or 4-story building were tested at the University of Washington (see Fig. 3a), and six 2- and 3-story full-scale SCBF frames (see Fig. 3c) were tested at the National Center for Earthquake Engineering (NCREE) Laboratory in Taiwan. These experiments evaluated a range of gusset plate connection design parameters including:

- The current AISC design procedures.
- The range of different failure modes possible for SCBF gusset plate connections.
- The impact of different brace cross sections, configurations, and orientations.
- Different connections (e.g., bolted and welded) between the gusset plate and framing members.
- Differences between the $2t_p$ linear clearance and alternate clearance models to achieve brace end rotation.
- The gusset plate thickness and resulting relative strength and stiffness of the brace, gusset and framing members.
- Variations in performance of tapered and rectangular gusset plates.
- Design requirements for both corner and midspan gusset plates.

Several additional tests were performed at the University of California (Berkeley) and the University of Minnesota NEES Laboratories, but the analysis of the data from these tests is incomplete and not included here. These tests realistically simulated the demands, capacities, and performance of the gusset plate connections, and the results of tests most relevant to gusset plate design are summarized in Table 1. The specimens were subjected to a cyclic inelastic deformation history based on the ATC-24 testing protocol, although a few tests employed a near-fault deformation history. The total drift range for each story as defined in Fig. 5 was used as the best indicator of system deformation capacity. Specimens with HSS and WF in the identifier had rectangular HSS tube and wide flange braces, respectively. Specimens identified as TCBF1 and TCBF2 specimens were two and three story specimens tested at the NCREE Laboratory in Taiwan.

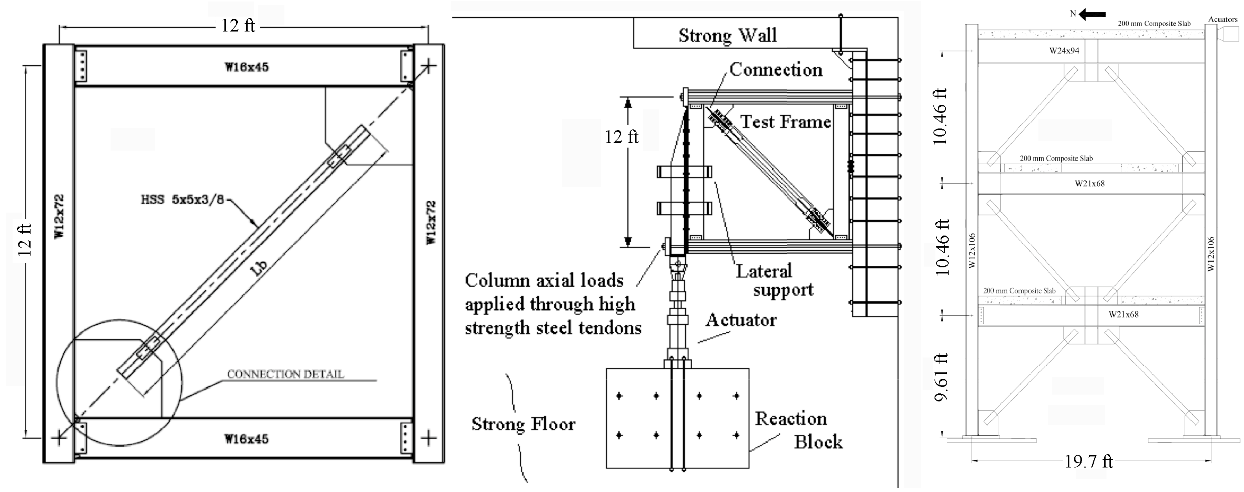

a) Typical Single Story Specimen b) Single Story Setup c) Typical 3-Story Specimen

Figure 4. Test Specimens and Setup

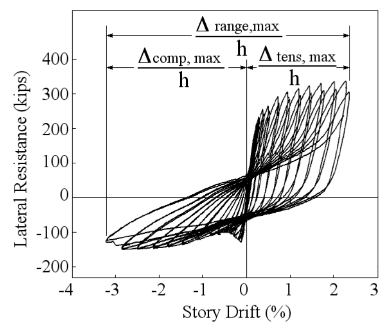

Figure 5. Definition of Drift Range

The single story-single bay frames include the brace, beams, gusset plate connections at each end of the brace, and columns to complete the single bay frame assembly as shown in Fig. 4a. They are tested in a horizontal position with the apparatus shown in Fig. 4b. The goal of the research was to evaluate SCBF gusset plate connections, and therefore most specimens had HSS 5x5x$^{3}/_{8}$ inch tubes, A992 W12x72 columns, and A992 W16x45 beams. Other sections were used for a few specimens for specific test goals. Similar member sizes were used for most tests, because a primary goal of the research was evaluation of different gusset plate connection design strategies. The two and three story frames had somewhat different member sizes as illustrated in Fig. 4c. The complete test results are lengthy and cannot be comprehensively discussed here, but more detailed information is available elsewhere (Johnson, 2005; Herman, 2007; Kotulka 2007, Powell 2010, Kelly 2009, and Lumpkin 2010). However, several key tests are summarized here to illustrate important differences and observations.

Figure 6 shows the details of four gusset plate connections, and Fig. 7 shows the force-deflection behavior for these same specimens. Specimen HSS1 was designed using the current AISC UFM method with the commonly used $2t_p$ clearance method as shown in Fig 6a. Figure 7a shows that the ductility of this specimen was limited as a result of weld fracture of the fillet welds joining the gusset plate to the beam and column as shown in the photo of Fig. 8a. This weld fracture initiated as ductile weld tearing, but abrupt fracture occurred as the weld cracks grew to significant length. The welds were AISC demand critical welds. These research results show that the gusset plate welds must develop the plastic capacity of the gusset plate rather than the expected plastic capacity of the brace, because extensive yielding must be expected in the gusset plate during severe earthquakes regardless of the gusset plate thickness. The $2t_p$ buckling clearance normal to the axis of the brace results in relatively large plates, and the relatively large stiff, nearly rigid zone that forces significant local yield deformation in the beam and column adjacent to the gusset. Alternate clearance methods were considered, and the elliptical clearance method illustrated in Fig. 9a was evaluated as an improved, alternate design method for corner gussets and was used for Specimens HSS5, HSS10 and HSS11.

Table 1. Summary of Test Program

Specimen Brace Type	Specimen Description	Gusset and Clearance	Failure Mode	Drift Range %
HSS-1	AISC Design – fillet welds by UFM.	13mm – $2t_p$ linear	Weld fracture	2.8
HSS-2	HSS1 w/fillet weld sized to cap. of plate	13mm – $6t_p$ ellipse	Brace fracture	4.0
HSS-3	BDP-Fillet weld sized to capacity of plate	13mm - $6t_p$ ellipse	Brace fracture	5.0
HSS-4	BDP-Fillet weld sized to capacity of plate	13mm – $9.4t_p$ ellipse	Brace fracture	4.8
HSS-5	BDP-Fillet weld sized to capacity of plate	10mm – $8t_p$ ellipse	Brace fracture	5.5
HSS-6	BDP-HSS5 except fillet welds reinforced	10mm – $8t_p$ ellipse	Brace fracture	4.8
HSS-7	BDP-Fillet weld sized to capacity of plate	22mm – $6t_p$ ellipse	Brace fracture	4.0
HSS-8	BDP-Fillet weld sized to capacity of plate	10mm – $3t_p$ ellipse	Brace fracture	4.6
HSS-9	BDP-CJP weld	13mm – $6t_p$ ellipse	Brace fracture	3.7
HSS-10	BDP-Tapered gusset – fillet welds to plate cap.	13mm – $7t_p$ ellipse	Brace fracture	4.5
HSS-11	Heavy beam –fillet welds to plate capacity	22mm – $6t_p$ ellipse	Brace fracture	2.6
HSS-12	AISC Design - CJP weld	13mm – $2t_p$ linear	Brace fracture	3.5
HSS-13	BDP-CJP weld	13mm – $7t_p$ ellipse	Brace fracture	4.1
HSS-14	No net section reinf – fillet welds to pl. cap.	10mm – $8t_p$ ellipse	Brace fracture	3.9
HSS-15	BDP-Min. block shear – fillet welds to pl. cap.	10mm – $6t_p$ ellipse	Brace fracture	4.1
HSS-17	BDP-Tapered gusset – fillet welds to plate cap.	10mm – $9t_p$ ellipse	Brace fracture	4.9
HSS-18	BDP-Bolted shear pl. - fillet welds to plate cap.	10mm – $8t_p$ ellipse	Brace fracture	4.2
HSS-20	BDP-Bolted end plate	10mm – $7t_p$ ellipse	Brace fracture	4.0
HSS-21	BDP-Bolted end plate	10mm – $7t_p$ ellipse	Bolt fracture	4.2
HSS-22	BDP-Tapered gusset - unwelded beam flanges	10mm – $8t_p$ ellipse	Gusset tearing	4.0
WF-23	BDP-W6x25 wide flange brace	10mm – $8t_p$ ellipse	Weld fracture	5.6
HSS-24	BDP-3/8" gusset, 6 t_p elliptical	10mm – $8t_p$ ellipse	Brace fracture	4.4
HSS-25	Heavy beam – No net section reinf. – CJP weld	22mm – $6t_p$ ellipse	Brace fracture	3.3
HSS-26	Heavy beam – No net section reinf. - Near fault	22mm – $6t_p$ ellipse	Net section	1.7
HSS-27	No net section reinforcement - Near fault	10mm – $8t_p$ ellipse	Net section	2.5
HSS-28	BDP-Tapered gusset	19mm - $2t_p$ linear	Brace fracture	4.7
TCBF1-HSS	BDP-Two story	10mm – $8t_p$ ellipse	Brace fracture	4.3 Avg.
TCBF1-WF	BDP-Two story	10mm – $8t_p$ ellipse	Brace fracture	6.2 Avg.
TCBF1-T	BDP-Two story – Tapered gusset	20mm - $2t_p$ linear	Brace fracture	5.6 Avg.
TCBF2-HSS	BDP-Three story	10mm - Varies	Brace fracture	3.8 Avg.
TCBF2-WF	BDP-Three story	10mm - Varies	Brace fracture	4.9 Avg.
TCBF2-IP	BDP-Three story – In plane buckling	20mm - $2t_p$ linear	Brace fracture.	3.5 Avg.

The elliptical clearance was based on observed yielding of the gusset plate in experiments (see Figs. 10a) and nonlinear FE analysis, which demonstrated similar stress and deformation patterns (see Fig. 10b) (Yoo, 2006). The elliptical shape is both consistent with these observations, and readily usable in both graphical and mathematical form by design engineers. Specimen HSS5 (and most other specimens in the test matrix) used this elliptical clearance and had welds that were designed to develop the full plastic capacity of the gusset plate. The clearance limit (nt_p) used alternate values of "n" as shown in Table 1. The elliptical clearance model and clearance limits in the order of $6t_p$ to $8t_p$ provided increased deformation capacity and had adequate resistance to develop the brace force with little excess resistance. Figures 6b and 7b show the connection details and force-deflection behavior for Specimen HSS5, which attained much larger ductility and inelastic deformation capacity than HSS1. The brace of HSS5 experienced large out-of-plane deformation seen in the photo of Fig. 8b and ultimately fractured at the center of the buckled region as illustrated in Fig. 8c.

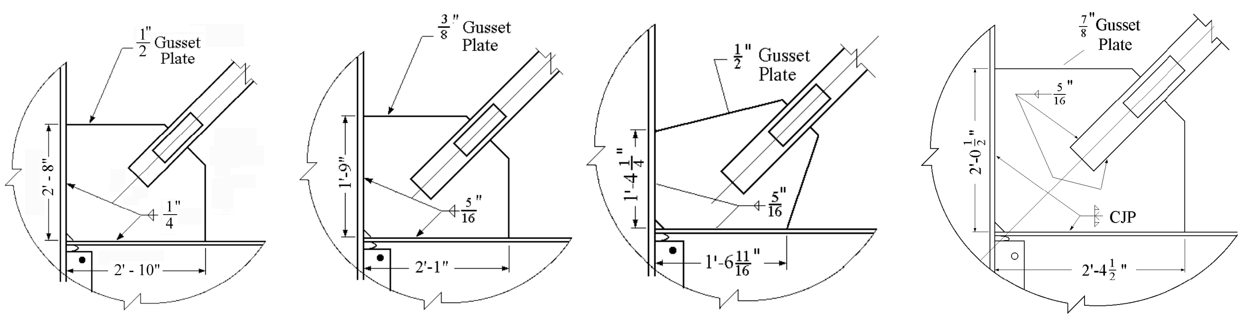

a) b) c) d)

Figure 6. Gusset plate design; a) HSS1, b) HSS5, c) HSS10, and d) HSS11

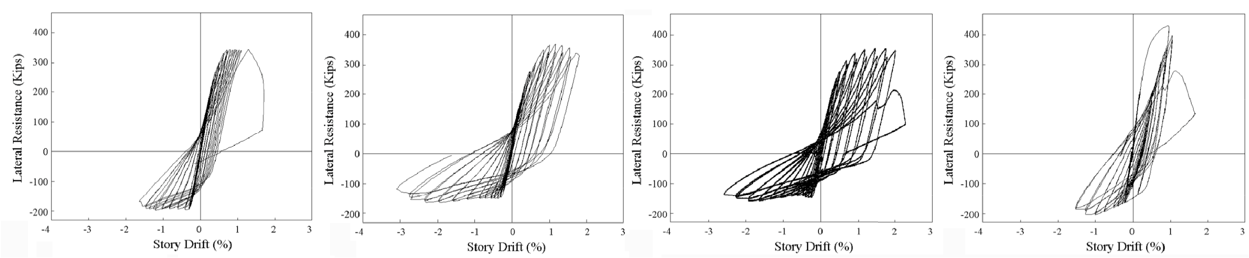

a) b) c) d)

Figure 7. Cyclic force-deflection behaviors; a) HSS1, b) HSS5, c) HSS10, and d) HSS11

Specimen HSS10 had a tapered gusset plate connection as shown in Fig. 6c. Tapered gusset plates create a smaller stiff corner for the beam column connection, and the elliptical clearance model with a $6t_p$ to $8t_p$ elliptical clearance limit is similar to the $2t_p$ linear clearance limit for connections with significant taper. Figure 7c shows that tapered gussets are capable of achieving good SCBF ductility. They provide good end rotation capability for the brace, and the brace can attain large out-of-plane deformation before localization of damage and brace fracture. However, there are also limitations with the tapered gusset plate connection. The tapered gusset provides a Whitmore width that often exceeds the true width of the gusset, therefore they have less reserve axial and bending resistance than rectangular gussets. Earlier and greater inelastic deformation must be expected in tapered gusset plates and the gusset plate welds, unless thicker gussets and larger welds are employed, but these thicker gussets have negative consequences. This can be verified by comparing the performance of specimens HSS10 and HSS13. The force-deflection behavior of HSS10 is shown in Fig. 7c. It can be seen that the specimen developed good inelastic deformation capacity for the frame, but not shown in the figure is the observation that weld cracking and the plastic deformation of the gusset were significantly greater for this specimen than for other tests. Specimen HSS13 was similar to HSS10 except that it used a thicker gusset plate and CJP weld to minimize the damage noted in HSS10. The force-deflection behavior is not shown for this specimen, but the inelastic deformation capacity of this connection was significantly smaller than that achieved for HSS10 because of the resulting increase in connection stiffness.

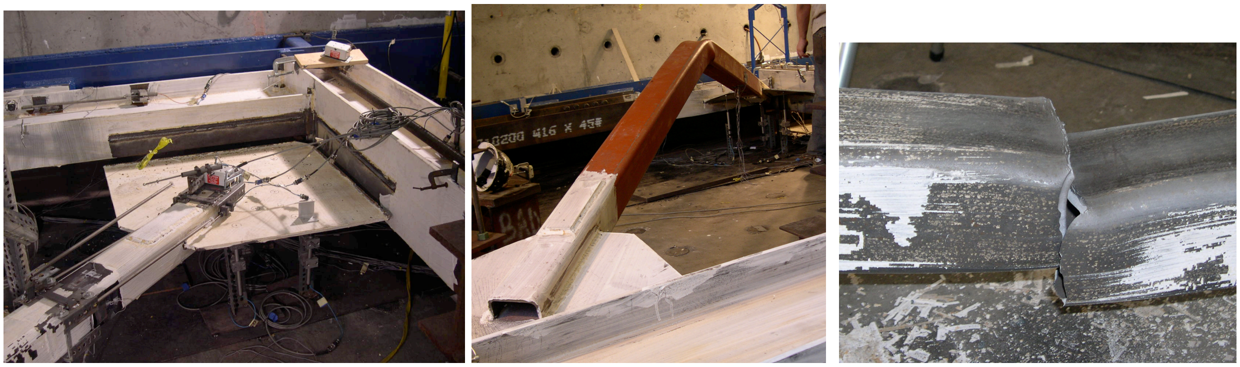

a) b) c)

Figure 8. Photographs of test results; a) Weld fracture of HSS1, b) Large out-of-plane buckling deformation of HSS5, c) Brace fracture

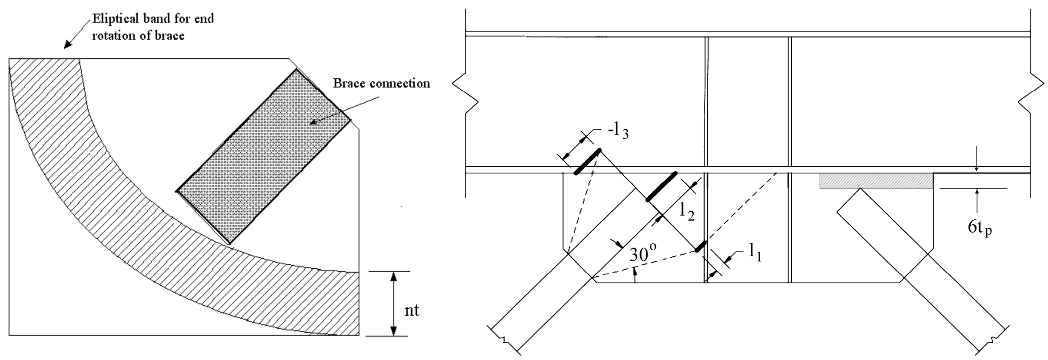

a) b)

Figure 9. Recommended Clearance Models; a) Elliptical Model for Corner Gussets, b) Linear Band for Midspan Gussets

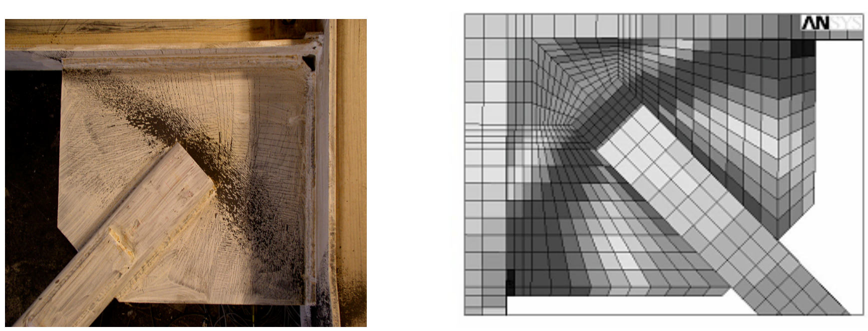

a) SCBF test (b) FE analysis for SCBF

Figure 10. Elliptical Hinge Line Pattern and Stress Distribution

Figure 6d shows that Specimen HSS11 had a thick gusset plate and a W16x89 beam to increase the connection strength and stiffness. The connection and framing members were significantly stiffer and stronger than required to develop the inelastic performance of the brace. Figure 7d shows its force deflection behavior, and very limited ductility was achieved. Reduced deformation capacity occurred, because the thick gusset and heavy beam section concentrated the plastic strains into the center of the buckled brace. It also forces significant local yielding into the column. The out-of-plane deflection at brace fracture was much smaller than observed with HSS5 and other test specimens with more balanced connection design. The increased connection stiffness increased lateral resistance of the frame, because of the reduced effective length of the brace, but the reduction in inelastic deformation capacity has serious consequences to the system performance.

The two and three story frame tests at NCREE (series TCBF1 and TCBF2 tests) all had midspan gusset plates in addition to corner gussets, and the midspan gussets were a focus of these tests. The elliptical clearance model does not work well for midspan gusset plate connections, and alternate models were considered through the analytical and experimental research. A $6t_p$ vertical clearance zone, as shown in Fig. 9b, ultimately was developed for midspan gusset plates and was evaluated in Specimens TCBF2-1 and 2-2. This vertical clearance provides similar behavior to the elliptical clearance with corner gussets.

A number of observations were made from the experimental research, and a few key conclusions that relate to gusset plate connection design are noted here. These include:

1) Welds joining the gusset plate to the beam and column must be designed to achieve the plastic capacity of the gusset plate rather than the expected plastic capacity of the brace and the UFM.
2) The elliptical clearance model significantly increases the inelastic deformation capacity of rectangular gusset plates if the elliptical clearance (see Fig. 9a) is in the range of $6t_p$ to $8t_p$. It permits smaller, more compact gusset plates which reduces the size of the relatively rigid connection stiffness zone, and as a consequence reduce the damage to welds and the beam and column adjacent to the gusset plate. Smaller elliptical clearances increase inelastic demands on the gusset plate welds, and larger clearances lead to larger and stiffer gusset plates, which may result in earlier brace fracture. The vertical 6tp clearance band shown in Fig. 8b provides similar performance for midspan gusset plates.
3) Yielding in the Whitmore width of the gusset plate is a desirable yield mechanism if it starts after initiation of yielding and buckling of the brace. This yielding minimizes damage to the welds and reduces local yield deformation in the beams and columns.
4) The strength and stiffness of the gusset plate must be adequate to assure that the brace develops it full resistance and inelastic deformation capacity, but it should not have excessively large strength or stiffness, because they cause early brace fracture.
5) The effective length of the brace should be taken as the true brace length when these rules are employed.
6) Tapered gusset plates may provide good end rotational capacity for the brace, but they may result in thicker gussets or greater inelastic demands on the gusset plate and the welds.

PROPOSED DESIGN METHOD

A rational design procedure is proposed to incorporate these design concepts and improve the seismic performance of SCBF gusset plate connections (Roeder et al. 2012). The design method utilizes the $8t_p$ elliptical clearance model shown in Fig. 9a for corner gusset plates and the $6t_p$ vertical clearance band shown in Fig. 9b for midspan gusset plates. These clearance models establish the basic size and geometry of the connection. Plate thickness, weld size, and other gusset requirements are determined from yield mechanisms and failure modes as illustrated in Fig. 11. A balanced design procedure, which is similar to current design methods in that the framing elements are designed to meet the force demands, and which utilizes the expected tensile yield ($R_yF_yA_g$) and compressive buckling ($R_yF_{cr}A_g$) capacities of the brace for design, is proposed.

Elliptical Clearance Model

Corner gusset plates utilize the elliptical clearance model. The geometry can be established by graphical methods, but a theoretical approach utilizing the geometry shown on Fig. 12a has been proposed (Lehman et al 2008). The dimensions a and b are selected so that the imaginary corner of the gusset plate intersects the centroidal axis of the brace as shown in the figure. The radii of the ellipse, a' and b', are then established by:

$$a' = a - 8t_p \tag{1a}$$
$$b' = b - 8t_p \tag{1b}$$

and the aspect ratio of the ellipse is

$$\rho = \frac{a'}{b'} \tag{2}$$

The dimensions, *x'* and y', define the exact intersection of the centroidal axis of the brace with the elliptical shape.

$$y' = a' \sin\left(\tan^{-1}\left(\rho \tan(\alpha)\right)\right) \tag{3a}$$

$$x' = a' \sqrt{1 - \left(\frac{y'}{b'}\right)^2} \tag{3b}$$

where α is the angle of inclination of the brace. However, the entire brace cross section must remain clear of the elliptical zone, and a correction, Corr, is applied to the dimensions to achieve this adjustment.

$$\beta = \tan^{-1}\left(\frac{-2}{\rho}\sqrt{\frac{a'^2}{x'^2}}\right) \tag{4a}$$

$$Corr = c \sin(\beta)\cos(\alpha) \tag{4b}$$

$$l' = \sqrt{x'^2 + y'^2} + Corr \tag{4c}$$

The dimension *c* is the maximum distance from the centroidal axis to the extreme fiber of the brace, and l' is the length of the brace from the imaginary gusset corner needed to assure the $8t_p$ clearance zone. This is an approximate solution, but the solution has been checked for different geometries and the potential error is small.

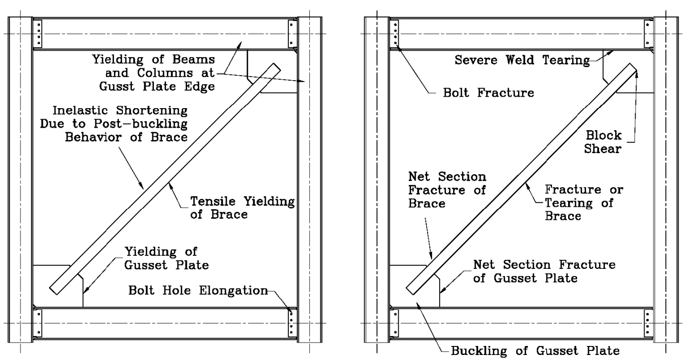

Figure 11. Typical behaviors for SCBFs; a) Yield mechanisms, b) Failure modes

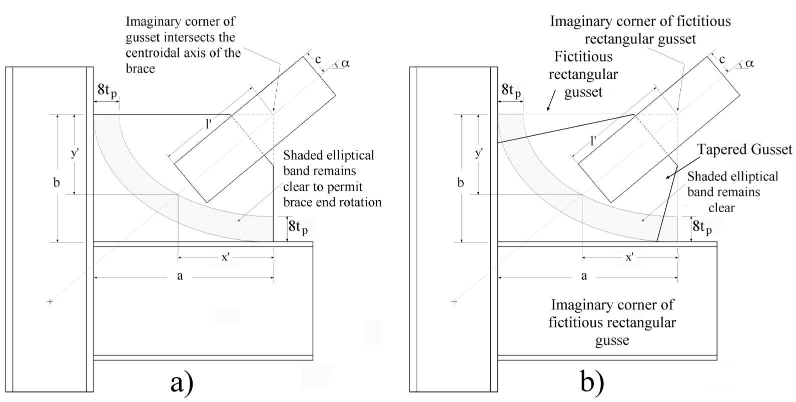

Figure 12. Application of Elliptical Clearance Model, a) Rectangular Gussets, b) Tapered Gussets

The elliptical clearance can be defined for tapered gusset plates by the fictitious geometry provided in Fig. 12b. A fictitious rectangular gusset is defined by the lighter lines in the figure, and resulting the a and b dimensions are used to establish the l' for the tapered gusset by equations 1 through 4. The $2t_p$ linear clearance model and the $8t_p$ elliptical clearance method produce similar gusset clearance geometry for tapered gussets with significant taper angle. For midspan gussets the horizontal clearance zone of $6t_p$ vertical height can be determined directly from Fig. 9b.

Balance Design Procedure

All yield mechanisms and failure modes for the SCBF gusset plate connections are evaluated by a balanced design procedure. Increased ductility is achieved with the proposed method by assuring that multiple, desirable yield mechanisms are developed prior to fracture or failure of the connection. This process satisfies serviceability design limits, since all members have resistance greater than the expected plastic resistances of these members. This is accomplished by balancing the resistances associated with the yield mechanisms, as illustrated in Eq. 5a:

$$(R_yF_yA_g \text{ or } R_yF_{cr}A_g) \le \beta_{yield1}R_yR_{yield,1} \le \beta_{yield\,2}R_yR_{yield,2} \dots \le \beta_{yield\,i}R_yR_{yield,i} \tag{5a}$$

Eq. 5b is the failure mode balance procedure:

$$R_{yield\ mean} = R_yR_{yield} < \beta_{fail,1}R_{fail,1} < \beta_{fail,2}R_{fail,2} \ \dots \text{ and } \beta_{yield} < \beta_{fail} \tag{5b}$$

The subscripts 1, 2, 3 etc. reflect the preferred sequence of yielding and the less desirable failure modes. Smaller β values are used for less ductile yield mechanisms and less desirable failure modes. In these equations, R_y is the ratio of the expected yield stress to the specified yield stress and R_{yield} and R_{fail} are the nominal resistance values of the yield mechanisms and failure modes in question, respectively. A desirable sequence of yielding and the prevention of undesirable failure modes is achieved through the use of β factors as shown within these expressions. The β factors are similar to resistance factors, φ , used in AISC LRFD design (AISC 2005b), but they are based upon ductility and inelastic deformation capacity rather than a specified strength under statistically extreme loads. The yield mechanisms include R_y in the evaluation of resistance, but R_y is not considered in the failure mode resistance to assure conservative strength predictions. Each yield mechanism and failure mode has its own β factor, which was established by evaluation of the deformation capacity achieved from various design β values for that mode and mechanism in past experiments. This evaluation is described elsewhere, but Fig. 13 shows two typical evaluations completed during that research (Roeder et al. 2011). The β values are always less than or equal to 1.0, and they become increasingly small for less desirable yield mechanisms and failure modes. The desirability of various yield mechanisms and failure modes is evaluated based upon the inelastic deformation capacity achieved in past experiments with test specimens with different design β values as illustrated for two specific cases in Fig. 13.

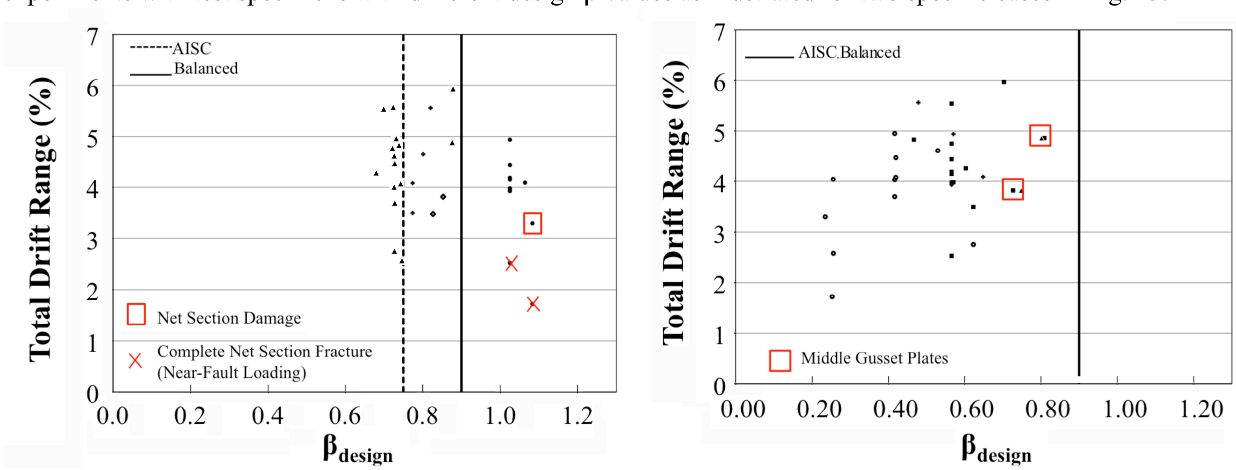

a) b)

Figure 13.Typical β value determinations; a) Net section of brace, b) Gusset plate buckling

The β values of Table 2 were determined from detailed evaluation of all possible yield mechanisms and failure modes (Roeder et al. 2011), and Fig. 13 illustrates two of these evaluations. Figure 13a shows the maximum inelastic deformation capacity achieved as a function of the design β value for the net section fraction of the brace. Most specimens had no visible net section damage even though many specimens had β values significantly greater than 1.0. The squares in the figure identify the 3 specimens that had some net-section damage or failure, and they had β factors greater than 1.0. The tests showed that net-section fracture is preceded by limited yield deformation, and larger β factors had increased system deformation capacity if net-section fracture is avoided. However, net-section fracture is sudden and results in complete loss of brace resistance, when it occurs, and the recommended β factor of 0.95 is conservative for mitigation of brace net-section fracture. This is significantly larger than the AISC LRFD ϕ factor of 0.75, and it reduces the amount of net section reinforcement required for good seismic performance. Figure 13b shows the ductility achieved as a function of the design β value for gusset plate buckling. A variation of the Thornton method is used to evaluate gusset plate buckling. The proposed method uses the Whitmore width to establish the area effective in buckling, and a average buckling length, L_{avg}, of the three buckling lengths (L_1, L_2, L_3), as illustrated in Fig. 9b. Negative lengths are used in the proposed evaluation as shown in the figure. This is different than the original Thornton method, but it provides consistent results these test results. The effective length coefficient was 0.65 for the corner gusset plates with the elliptical clearance model and 1.5 for midspan gussets designed by the 6tp horizontal clearance. The AISC column provisions are used to determine the critical buckling stress, F_{cr}. None of the specimens exhibited gusset plate buckling, and specimens with larger β factors showed somewhat greater inelastic deformation capacity. However, the figure shows that these tests did not place severe demands on the AISC buckling design provisions, and therefore the balance factor, β, factor for GP buckling is 0.9, which is the same valuse as the ϕ factor for AISC LRFD compression member design.

Table 2 summarizes the evaluation equations and β factors for all yield mechanisms and failure methods for SCBF gusset plate connection design.

Table 2: Limit States and Resistance Expressions by AISC and Balanced Design Approaches

Limit State	Balanced Design		Notes
	Resistance (βR_n)	**β**	
Whitmore Yielding	$\beta R_y F_y B_w t_p$	1.0	Preferred yield mechanisms and yielding is strongly encouraged.
Brace Net Section Fracture	$\beta U(R_{tb} F_{ub} A_{nb} + F_{up} A_{gp})$	0.95	Provides limited ductility, and net section failures related to specific loading hence larger β.
Brace to Gusset Weld	$\beta(0.6)F_{EXX} N_w L_c (.707) w_2$	0.75	Identical to AISC requirements.
Brace to Gusset Base Metal	$\beta(0.6)F_u N_s L_c t_f$	0.75	Identical to AISC requirements.
Block Shear	$\beta\{(0.6F_u A_{nv} + U_{bs} F_u A_{nt})$	0.85	Approximates one of two equations used in AISC provision.
Whitmore Fracture	$\beta F_u B_w t_p$	0.85	A more conservative requirement may be required for bolted joints.
Gusset Plate Buckling	$\beta B_w t_p F_{cr}$	0.90	Average gusset length of gusset with K of 0.65 for corner gussets and 1.5 for midspan gussets
Interface Welds	$2(1.2)\beta(0.6)F_{EXX}(.707)w_1 \geq R_y F_y t_p$	0.75	Considers increased capacity of fillet welds in transverse tension and matches the tensile yield of gusset.

ANALYTICAL STUDY

The application of this balanced design procedure has been shown to increase the inelastic deformation capacity of SCBFs by an average 46%. A wide range of nonlinear finite element (FE) analyses were performed with the ANSYS (2005) computer program to support the experimental program and develop the design procedure (Yoo, 2006). These analyses employed fine mesh quadrilateral shell elements including large-deflection formulations with geometric stiffness and bilinear kinematic plastic hardening material behavior as shown in Fig. 15a. Nonlinear spring models were used to model bolted web connections. The analyses were compared to experimental results for all tests shown in Table 1, and the comparison between experiments and analyses were very good at both the global performance and local deformation levels (Yoo et al, 2007). Figure 15b illustrates a typical comparison of the global force deflection response for one test specimen, and Figs. 10 and15c show typical comparisons of local behavior. A comprehensive series of nonlinear dynamic analysis was also performed with the OpenSees computer program.

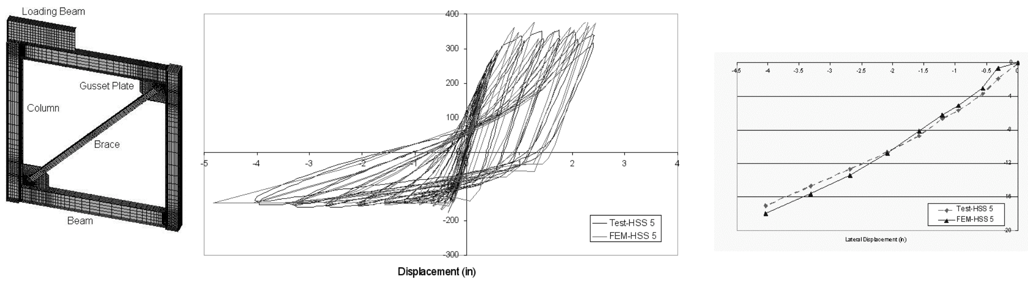

a) FEM Model b) Global Comparison of Measured and Computed Behavior c) Local Comparison of Measured and Computed Behavior

Figure 15. Nonlinear computer analysis of CBFs with ANSYS

The OpenSees computer program provides nonlinear analysis capabilities with relatively simple models that are formed by fiber elements, and progression of global yielding and buckling can be predicted with reasonable accuracy. These models will not capture local buckling or some other local deformations that can be predicted with the ANSYS analysis models, but nonlinear time history analysis of seismic response can be completed quickly and efficiently. However, the modeling procedures are still extremely important as illustrated in Figs. 16 and 17 (Hsiao et al. 2011). Figures 16a and b show relatively simple OpenSees models as may be commonly used in practice. Figures 16a and 17a show a FEM model and the analytical comparison to experimental results where the members are formed as line elements and the joints are pinned as in an idealized truss. The maximum resistance with the brace in compression is underestimated by more than 20% with this model, and the predicted resistance increases after brace buckling, while post-buckling stiffness and deformation are also poorly predicted. Some engineers recognize the gusset plate connections create a relatively rigid joint, and so rigid connections may be employed as illustrated in Figs. 16b and 17b. Rigid gusset connections overestimate the frame resistance with the brace in compression, underestimate the resistance with the brace in tension, and provide poor simulation of the force-deflection behavior at large inelastic deformations.

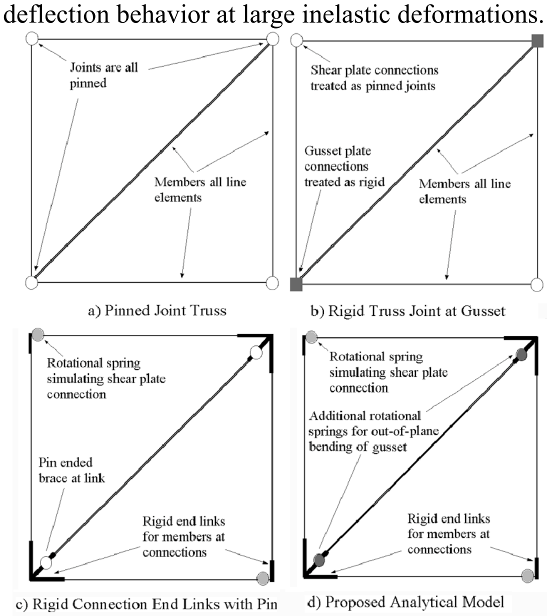

Figure 16. Comparison of OpenSees Models

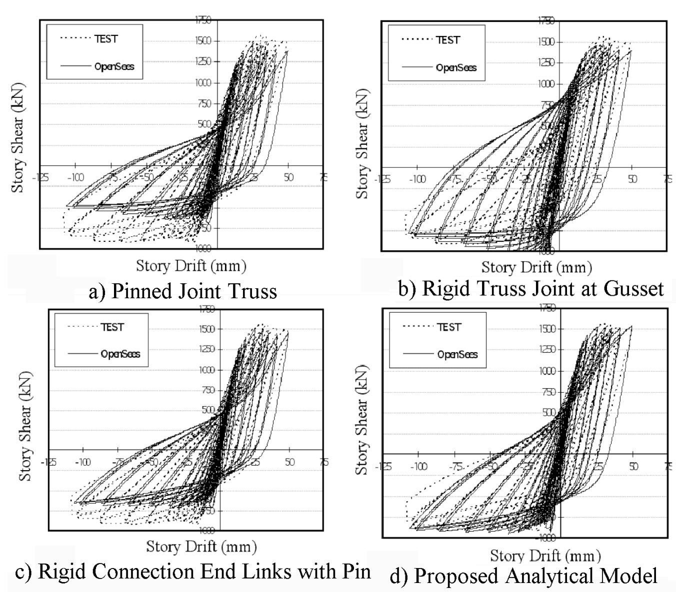

Figure 17. Comparison of OpenSees Results and Experiments

Figure 16c shows a more refined model, which recognizes that the beams, columns, and gussets have finite dimensions, and rigid links are used to represent the large stiffness in the gusset region. Nonlinear rotational springs simulate the rotational restraint provided by gusset plate deformation and shear plate connections. Figure 17c shows that this model underestimates the resistance of the frame by nearly 30%. Finally, the modified model in Fig. 16d is identical to the model of Fig. 16c except that a nonlinear rotational spring was added to reflect the bending stiffness and resistance of the gusset for end rotation of the brace. The nonlinear properties of the spring are based upon the dimensions and material properties of the gusset plate and shear plate connections. This model provides a very good estimate of the CBF resistance with the brace in tension and compression at all deformation levels as shown in Fig. 17d, and it provides a better representation of the cyclic inelastic behavior at large frame deformations. Both refined models overestimate the frame stiffness during the unloading cycles of the brace after large frame deformations, because fiber models do not simulate the localization of buckling damage noted with rectangular HSS braces at large frame deformations. Similar comparisons were achieved with all test specimens, and the model in Fig. 16d consistently provides more accurate simulation of CBF performance.

This model was further modified to predict brace fracture, and this adaptation permitted continuation of the frame analysis beyond initial fracture of the brace or connection and estimation of structural collapse. The brace fracture model was based upon strain history in the severely strained region of the brace, and the strain limit was determined from and calibrated to brace fracture test results. The resulting model was combined with other models including the stiffness and resistance of gravity framing, and the combination of these models were used to perform a large number of nonlinear dynamic analyses on a wide range of braced frame systems. Several SCBFs were designed for Seattle, WA with the balanced design approach noted earlier. Alternate braced frames using reduced response modification factors (R values) were also evaluated with the current SCBF provisions and the balanced design procedures. Twenty acceleration records were selected to be appropriate for Seattle response spectra with each of 2% and 10% probability of exceedance in 50 years. The results of these analyses were then used to estimate the probability of achieving brace buckling, brace fracture or potential structural collapse for a given seismic hazard. These results are summarized in Fig. 18. The SCBF designed with the current R=6 has a 95% probability of brace buckling but no risk of brace fracture or collapse during the more frequent event. During a 2% in 50 year event, the SCBF has a 25% probability of brace fracture. A reduction in response modification factor (R value) is often proposed as a method of reducing seismic damage and collapse potential, and the figure demonstrates the effect of reducing or increasing the R value for these seismic events. A reduction in the R value nominally results in an increase in lateral resistance of the system. The reduction in R value reduces the probability of brace buckling somewhat, but there is still a high probability of brace buckling even with R=3 in the 500 year event. The reduced R value also reduces the probability of brace fracture and potential collapse during the 2% in 50 year event, but the benefit may be somewhat smaller than expected. Ductile detailing requirements clearly have greater impact than increased seismic resistance. While the 15% probability of collapse for SCBFs in the 2% in 50 year event may be an issue of concern, it must be recognized that a 2500 year earthquake is quite extreme and all structural systems have a measurable probability of collapse during these extreme events.

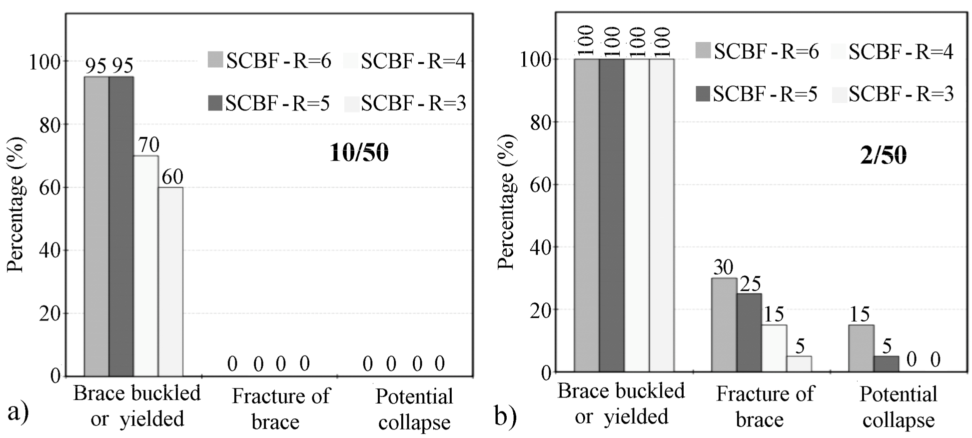

Figure 18. Results of Nonlinear Dynamic Analyses of 3 Story CBFs in Seattle;

Nine and 20 story buildings were also analyzed, but the results are not shown in the figure. However, the probability of brace buckling, brace fracture and potential collapse are significantly reduced with taller structures. These calculations are not intended to be a definitive evaluation of the seismic design method, but they demonstrate that good seismic performance can be achieved for all performance levels. The damage potential is clearly greater for shorter buildings, but with good ductile detailing practices the seismic performance of the building can significantly reduce seismic risk.

While OpenSees is a simpler form of nonlinear analysis than the continuum analysis shown in Fig. 15, it is still more complex than preferred by most structural engineers. Nevertheless, this analysis provides reasonable accuracy and demonstrates the importance of accurate modeling for reliable prediction of the seismic performance of braced frames. Further, the OpenSees analysis is a valuable research tool, which can address many global issues for braced frame design. Research continues on many of these issues, including important issues about seismic design criteria and the potential for concentration of inelastic deformation into a single story after brace buckling.

SUMMARY AND CONCLUSIONS

A brief summary of recent research on SCBF systems has been provided. Experimental and analytical research on the system has shown that the system performance is strongly dependent on system behavior. Component tests are helpful in assessing design provisions, but the true seismic performance depends upon the total system of members and connections. The brace is clearly the dominant member in braced frame systems, but significant local damage must be expected in the beams, columns and gusset plate connections. Gusset plate connections have been evaluated and a new balanced design procedure has proposed to improve seismic performance. An improved elliptical clearance method has been proposed as a method to permit brace end rotation due to brace buckling. The combination of these improvements has led to a demonstrated 46% increase in the inelastic deformation capacity that can be achieved with the SCBF system. Nonlinear analyses have also been performed on the SCBF system to support the experimental research program and to facilitate nonlinear dynamic analysis of SCBFs. The analytical models are compared to experimental results to verify their accuracy and reliability. The results of these analyses demonstrate the importance of accurate modeling of the SCBF system including all members and connections. The importance of the simulation of the connection is shown, and the best models are used to predict the seismic response under earthquake accelerations. The results show that SCBFs can provide good seismic performance at all hazard levels. It is shown that shorter buildings have a higher probability of greater seismic damage and collapse potential, because these older structures were built without ductile detailing requirements currently required for SCBF design. Increased seismic resistance may reduce the seismic damage, but the greatest benefit to seismic performance is achieved through improved inelastic performance of the system.

ACKNOWLEDGEMENTS

This research was funded by the National Science Foundation under grants CMS-0301792, Performance-Based Design of Concentrically Braced Frames and CMS-0619161, NEESR-SG International Hybrid Simulation of Tomorrow's Braced Frames. Supplemental funding was provided by AISC. International testing, fabrication and collaboration was conducted at the NCREE Laboratory in Taiwan with Dr. Keh-Chyuan Tsai, Laboratory Director. Frequent advice and guidance was provided through the research Advisory Group, composed of Tom Schlafly (AISC), Tim Fraser (CANRON), Walterio Lopez (Rutherford and Chekene), Larry Muir (CIVES) and Rafael Sabelli (Walter P. Moore). The advice and financial support of these individuals and institutions is greatly appreciated.

REFERENCES

AISC (2001) "Manual of Steel Construction, Load and Resistance Factor Design," 3rd Edition, American Institute of Steel Construction, Chicago, IL.

AISC (2005b) "Manual of Steel Construction," 13th Edition, American Institute of Steel Construction, Chicago, IL.

Astaneh-Asl, A., (1989) " Simple Methods for Design of Steel Gusset Plates," Proceedings ASCE Structures Conference, San Francisco, CA.

Bjorhovde, R., and Chakrabarti, S.K., (1985) "Test of Full Size Gusset Plate Connections," ASCE, *Journal of Structural Engineering*, Vol 111, No. 3, pg 667-84.

Brown, V.L.S., (1988) " Stability of Gusseted Connections in Steel Structures," A thesis submitted in partial fulfillment of Doctor of Philosophy in Civil Engineering, University of Delaware.

Cheng, J.J.R, Yam, M.C.H., and Hu, S.Z, (1994) "Elastic Buckling Strength of Gusset Plate Connections," Journal of Structural Engineering, Vol. 120, No. 2,

Grondin, G.Y, Nast, T.E., and Cheng, J.J.R., (2000) " Strength and Stability of Corner Gusset Plates Under Cyclic Loading, Proceedings of Annual Technical Session and Meeting, Structural Stability Research Council.

Herman, D. (2007) a thesis submitted in partial fulfillment of the Master of Science Degree at the University of Washington, Seattle, WA.

Hsiao, P-C, Lehman, D.E. and Roeder, C.W., (2011) "Improved Analytical Models for Special Concentrically Braced Frames," submitted for publication review, *Engineering Structures*, Elsevier.

Hu, S.Z., and Cheng, J.J.R., (1987) "Compressive Behavior of Gusset Plate Connections," Structural Engineering Report No. 153, University of Alberta, Canada.

Kotulka, B. (2007) a thesis submitted in partial fulfillment of the Master of Science Degree at the University of Washington, Seattle, WA.

Lehman, D.E., Roeder, C.W., Herman, D., Johnson, S., and Kotulka, B., (2007) "Improved Seismic Performance of Gusset Plate Connections," submitted for publication review, ASCE, *Journal of Structural Engineering*, Reston, VA.

Popov, E.P. Takanashi, K., and Roeder, C.W. (1976) Structural Steel Bracing Systems, EERC Report 76-17, University of California, Berkeley, 1976

Rabinovitch, J.S., and Cheng, J.J.R. (1993) "Cyclic Behavior of Steel Gusset Plate Connections," Structural Engineering Report No. 191, University of Alberta, Canada.

Roeder, C.W., Lehman, D.E., and Yoo, J.H. (2004) "Performance Based Seismic Design of Braced-Frame Connections, 7th Pacific Structural Steel Conference, Long Beach, CA, March 24-27, 2004.

Roeder, C.W., Lehman, D.E., and Yoo, J.H., (2005) "Improved Seismic Design of Steel Frame Connections," *International Journal of Steel Structures*, Korean Society of Steel Construction, Seoul, Korea, Vol. 5, No. 2, pgs 141-53

Roeder, C.W., Lumpkin, E.J., and Lehman, D.E. (2012) “Balanced Design Procedure for Special Concentrically Braced Frame Connections,” submitted for publication review, *Journal of Constructional Steel Research*, Elsevier.

Thornton, W.A., (1991) "On the Analysis and Design of Bracing Connections," AISC, *Proceedings of National Steel Construction Conference*, Section 26, pgs 1-33.

Tsai, K.C., (2003) Test results obtainable from the website, "http://cft-brbf.ncree.gov.tw/fs.html", for the National Center for Research in Earthquake Engineering, Taipei, Taiwan.

Yam, M.C.H., (1994) " Compressive Behavior and Strength of Steel Gusset Plate Connections," a thesis submitted in partial fulfillment of Doctor of Philosophy degree, University of Alberta, Canada.

Yam, M.C.H., and Cheng, J.J.R., (2002) "Behavior and Design of Gusset Plate Connections in Compression," *Journal of Constructional Steel Research*, Vol 58, No. 5-8, Elsevier, pgs 1143-59.

Yoo, J.H. (2006) “Analytical Investigation on the Seismic Performance of Special Concentrically Braced Frames”, a dissertation submitted in partial fulfillment of the Ph.D., University of Washington, Seattle, WA.

Whitmore, R.E., (1950) "Experimental Investigation of Stresses in Gusset Plates," a thesis submitted in partial fulfillment of the Master of Science Degree at the University of Tennessee, Knoxville, Tennessee.